Journal of Pharmaceutical Analysis 12 (2022) 683–691

Contents lists available at ScienceDirect

Journal of Pharmaceutical Analysis

journal homepage: www.elsevier.com/locate/jpa

Original article

Discovery of human pancreatic lipase inhibitors from root of *Rhodiola crenulata* via integrating bioactivity-guided fractionation, chemical profiling and biochemical assay

Li-Juan Ma [a, b, 1], Xu-Dong Hou [a, b, c, 1], Xiao-Ya Qin [a, 1], Rong-Jing He [a], Hao-Nan Yu [a], Qing Hu [a], Xiao-Qing Guan [a], Shou-Ning Jia [d], Jie Hou [c], Tao Lei [b, **], Guang-Bo Ge [a, *]

[a] *Shanghai Frontiers Science Center of TCM Chemical Biology, Institute of Interdisciplinary Integrative Medicine Research, Shanghai University of Traditional Chinese Medicine, Shanghai, 201203, China*
[b] *Department of Endocrinology, Putuo Hospital, Shanghai University of Traditional Chinese Medicine, Shanghai, 200062, China*
[c] *College of Basic Medical Sciences, Dalian Medical University, Dalian, 116044, China*
[d] *Qinghai Hospital of Traditional Chinese Medicine, Xining, 810099, China*

ARTICLE INFO

Article history:
Received 5 September 2021
Received in revised form
20 March 2022
Accepted 2 April 2022
Available online 8 April 2022

Keywords:
Human pancreatic lipase
Rhodiola crenulata
1,2,3,4,6-Penta-*O*-Galloyl-β-D-glucopyranose
Catechin gallate
Inhibitory mechanism

ABSTRACT

Although herbal medicines (HMs) are widely used in the prevention and treatment of obesity and obesity-associated disorders, the key constituents exhibiting anti-obesity activity and their molecular mechanisms are poorly understood. Recently, we assessed the inhibitory potentials of several HMs against human pancreatic lipase (hPL, a key therapeutic target for human obesity), among which the root-extract of *Rhodiola crenulata* (ERC) showed the most potent anti-hPL activity. In this study, we adopted an integrated strategy, involving bioactivity-guided fractionation techniques, chemical profiling, and biochemical assays, to identify the key anti-hPL constituents in ERC. Nine ERC fractions (retention time = 12.5–35 min), obtained using reverse-phase liquid chromatography, showed strong anti-hPL activity, while the major constituents in these bioactive fractions were subsequently identified using liquid chromatography-quadrupole time-of-flight mass spectrometry (LC-Q-TOF-MS/MS). Among the identified ERC constituents, 1,2,3,4,6-penta-*O*-galloyl-β-D-glucopyranose (PGG) and catechin gallate (CG) showed the most potent anti-hPL activity, with pIC_{50} values of 7.59 ± 0.03 and 7.68 ± 0.23, respectively. Further investigations revealed that PGG and CG potently inhibited hPL in a non-competitive manner, with inhibition constant (K_i) values of 0.012 and 0.082 μM, respectively. Collectively, our integrative analyses enabled us to efficiently identify and characterize the key anti-obesity constituents in ERC, as well as to elucidate their anti-hPL mechanisms. These findings provide convincing evidence in support of the anti-obesity and lipid-lowering properties of ERC.

© 2022 The Authors. Published by Elsevier B.V. on behalf of Xi'an Jiaotong University. This is an open access article under the CC BY-NC-ND license (http://creativecommons.org/licenses/by-nc-nd/4.0/).

1. Introduction

Obesity is regarded as a global public health problem, with the total number of overweight and obese adults estimated to be 1.9 billion and 650 million, respectively, in 2016 [1]. Accumulative evidence has indicated that obesity is closely associated with multiple metabolic disorders, including hyperlipidemia, hypertension, cardiovascular diseases, and numerous cancers [2–4]. Over the past few decades, the global incidence and mortality of obesity have risen sharply, and a diverse range of remedial strategies have been proposed for the prevention and treatment of obesity, including pharmacotherapy, dietary therapy, surgery, and behavioral therapy [5–7]. Among the proposed therapeutic strategies, herbal therapy has been widely used in the treatment of obesity-related disorders [8]. Many herbal medicines (HMs) have been reported to have significant anti-obesity activities, and some of them have been marketed as complementary and alternative medicines for treating obesity or obesity-related metabolic disorders [9–13]. However, in most cases, the key anti-obesity

Peer review under responsibility of Xi'an Jiaotong University.
* Corresponding author.
** Corresponding author.
E-mail addresses: leitao5899@126.com (T. Lei), geguangbo@dicp.ac.cn (G.-B. Ge).
[1] These authors contributed equally to this work.

https://doi.org/10.1016/j.jpha.2022.04.002
2095-1779/© 2022 The Authors. Published by Elsevier B.V. on behalf of Xi'an Jiaotong University. This is an open access article under the CC BY-NC-ND license (http://creativecommons.org/licenses/by-nc-nd/4.0/).

constituents in HMs and their molecular mechanisms of action are poorly illuminated.

In this context, it is worth noting that almost all constituents in HMs can directly interact with the targets in the gastrointestinal tract following oral administration, whereas very few constituents in HMs can be absorbed into the circulatory system and then perform their functions in the deeper organs (such as the liver) [14]. Thus, it is necessary to find the key constituents in HMs that can modulate the validated anti-obesity targets in the gastrointestinal tract [15–17]. Among all validated anti-obesity targets, pancreatic lipase (PL) plays a predominant role in the lipolysis of dietary triglycerides (the hydrolysis of 50%–70% of total dietary fats) [18]. It has been reported that significant dysfunction or strong inhibition of PL can effectively delay the digestion of dietary lipids [19,20]. In previous studies, a number of HMs, including *Cortex Mori*, *Ginkgo biloba*, *Fructus psoraleae*, and *St John's Wort*, have been found with potent anti-PL activity. Meanwhile, a range of bioactive natural compounds isolated from these herbs, including flavonoids, bioflavonoids, terpenoids, and phenolic compounds, have been identified as PL inhibitors [21–26]. Unfortunately, over the past few decades, most researchers have used commercially available porcine pancreatic lipase (pPL) to replace human pancreatic lipase (hPL) for in vitro PL inhibition assays. Although the amino acid sequence identity between hPL and pPL is relatively high (approximately 86%, Fig. S1), the PL obtained from these two mammalian species may differ in their response to certain reversible inhibitors [27,28]. Therefore, it is necessary to systematically screen herbal products showing potent anti-hPL activity and to identify the key constituents responsible for hPL inhibition.

Recently, we examined the inhibitory potentials of several HMs extracts against hPL and identified that the root extract of *Rhodiola crenulata* (ERC) had the most potent anti-hPL activity, with the residual activity of less than 5% at the dose of 100 μg/mL. Notably, several studies have reported that ERC can ameliorate irregular lipid metabolism in mammals by reducing the content of triglyceride in plasma [29]. This evidence combined with our preliminary results prompted us to explore the bioactive compounds in ERC and their anti-PL mechanisms. For this purpose, a panel of techniques including bioactivity-guided fractionation, liquid chromatography coupling with quadrupole time-of-flight tandem mass spectrometry (LC-Q-TOF-MS/MS)-based chemical profiling, and fluorescence-based biochemical assays were used to identify the key anti-hPL constituents in ERC. In addition, the inhibitory mechanisms of two potent hPL inhibitors, namely, 1,2,3,4,6-penta-*O*-galloyl-β-D-glucopyranose (PGG) and catechin gallate (CG), against hPL were explored by performing a series of inhibition kinetic analyses and docking simulations.

2. Material and methods

2.1. Chemicals

Seventy-three herbal extracts were provided by Jiangyin Tianjiang Pharmaceutical Co., Ltd. (Jiangyin, China). Further, 17 natural constituents identified from liquid chromatography (LC) fractions of ERC, namely, **1)** epicatechin, **2)** *p*-coumaric acid, **3)** ferulic acid, **4)** epicatechin gallate (ECG), **5)** catechin gallate (CG), **6)** 1,2,3,4,6-penta-*O*-galloyl-β-D-glucopyranose (PGG), **7)** luteolin-7-*O*-β-D-glucoside, **8)** afzelin, **9)** quercetin-3-*O*-glucoside, **10)** rhodiosin, **11)** quercetin-3-*O*-glucuronide, **12)** rhodionin, **13)** quercitrin, **14)** eriodictyol, **15)** quercetin, **16)** luteolin, and **17)** kaempferol, were obtained from Shanghai Standard Technology Co., Ltd. (Shanghai, China), and the purities were higher than 96%. The positive hPL inhibitor (orlistat, a commercial hPL inhibitor) was purchased from Dalian Meilun Biotech Co., Ltd. (Dalian, China). hPL was expressed and purified as described previously [30]. 4-methylumbelliferone (4-MU) was obtained from Sigma-Aldrich (Shanghai) Trading Co., Ltd. (Shanghai, China), and 4-methylumbelliferyl oleate (4-MUO) was purchased from J&K Scientific Co., Ltd. (Beijing, China). Liquid chromatography-mass spectrometry (LC-MS) grade formic acid, acetonitrile, methanol, and dimethyl sulfoxide (DMSO) were purchased from Thermo Fisher Scientific (Fair Lawn, NJ, USA).

2.2. hPL inhibition assay

A fluorescence-based assay was used to determine the residual activities of hPL in the presence or absence of any inhibitor, and orlistat was used as the positive control. In brief, incubation systems (total volume: 100 μL) were prepared by mixing 66 μL of Tris-HCl (pH 7.4, 25 mM), 20 μL of bile salt (0.1 mg/mL, final concentration), 10 μL of hPL (dissolved in Tris-HCl buffer, 0.25 μg/mL, final concentration), 2 μL of inhibitors (ERC and all other assessed compounds, dissolved in DMSO, 0–100 μM, final concentration range), and 2 μL of substrate (4-MUO, dissolved in DMSO, 5 μM, final concentration). Initially, the mixtures (with or without of inhibitors) were pre-incubated in Eppendorf tube (37 °C, 3 min). After the addition of 4-MUO, the mixtures were incubated (37 °C) for 20 min, then they were subjected to fluorescence analysis using a microplate reader (SpectraMax iD3, Molecular Devices, San Jose, CA, USA), with excitation and emission wavelengths of 340 and 460 nm, respectively. And the standard curve of 4-MU was plotted (Fig. S2). Reaction mixtures without inhibitors (DMSO only) were used as negative controls and were incubated under the same conditions. The residual activity of hPL was calculated using the following formula: the residual activity (%) = the fluorescence intensity of the test sample/the fluorescence intensity in the negative control (DMSO only).

2.3. Identification of bioactive fractions using an LC-MS-based fractionation strategy

In order to identify the ERC fractions with strong anti-hPL activity, a practical bioactivity and LC-MS-based fractionation strategy was employed. Briefly, an LC-MS-based fingerprint approach was established for separating the fractions derived from ERC. Subsequently, the LC fractions obtained at different time points were consecutively collected and their anti-hPL potencies were determined (Supplementary data 1). The compounds derived from these fractions were further analyzed using LC-Q-TOF-MS/MS (Supplementary data 2). After identifying the 17 constituents mentioned in Section 2.1 (the chemical structures are shown in Fig. S3), the inhibitory potentials were determined according to the protocol described in Section 2.2.

2.4. Inhibition kinetics of PGG and CG against hPL

Detailed molecular mechanisms of PGG and CG against hPL were executed using increasing concentrations of the substrate 4-MUO and multiple concentrations (0–80 μM) of the two inhibitors. In order to identify the inhibitory type (competitive, non-competitive, or mixed) and the inhibition constant (K_i), the inhibition kinetics analyses of the two inhibitors were performed. And K_i values were calculated as described previously [23,24,31–33].

2.5. Docking simulations

The Software of AutoDock Vina (version 1.1.2) was applied to explore the binding modes (non-competitive inhibition) of both PGG and CG in hPL [34], The crystal structure of hPL (1LPA) was obtained from the PDB website [35]. Initially, the interactive server platform (CavityPlus) was used for protein cavity detection and the

ligandability quantitaiton of the cavity binding sites [36]. Then, whole-protein docking between the two inhibitors and hPL was examined using Autodock Vina, which entailed the removal of both water molecules and irrelevant ligands, addition of hydrogen, merging of non-polar hydrogen atoms, and assignment of Kollman charges. Subsequently, the ligands (PGG or CG) and hPL were placed in AutoDock Tools with energy minimization. The docking modes with low binding free energies in the most excellent protein cavity were selected for further analysis.

2.6. Statistical analysis

All inhibition assays were performed in triplicate (three technical replicates) for each concentration of the inhibitors. pIC_{50} and K_i values were calculated using GraphPad Prism 7.0 (GraphPad Software, Inc., San Diego, CA, USA).

3. Results

3.1. Screening of the inhibitory activity of HMs against hPL

To identify HMs with potent anti-hPL activities, the inhibitory potentials of 73 HMs against hPL-mediated 4-MUO hydrolysis had been initially investigated. As shown in Fig. 1, seven HMs, namely, *Arnebia*, *Myristica fragrans*, *Glabrous greenbrier*, *Prunus Persica*, *Clove*, *Hawthorn*, and *Rhodiola crenulata* (*R. crenulata*), showed potent inhibitory activities against hPL, with residual activities of less than 20% at the dose of 100 μg/mL. Among all examined HMs, ERC showed the strongest hPL inhibition (residual activity<95%), and consequently, ERC was used for further analyses. Our results revealed that ERC inhibited hPL in a dose-dependent (IC_{50} = 0.1019 ± 0.0123 μg/mL) and time-independent manner (Fig. S4). The above results indicated that ERC contained naturally reversible hPL inhibitors, which prompted us to further identify the major bioactive constituents of ERC associated with the inhibition of hPL.

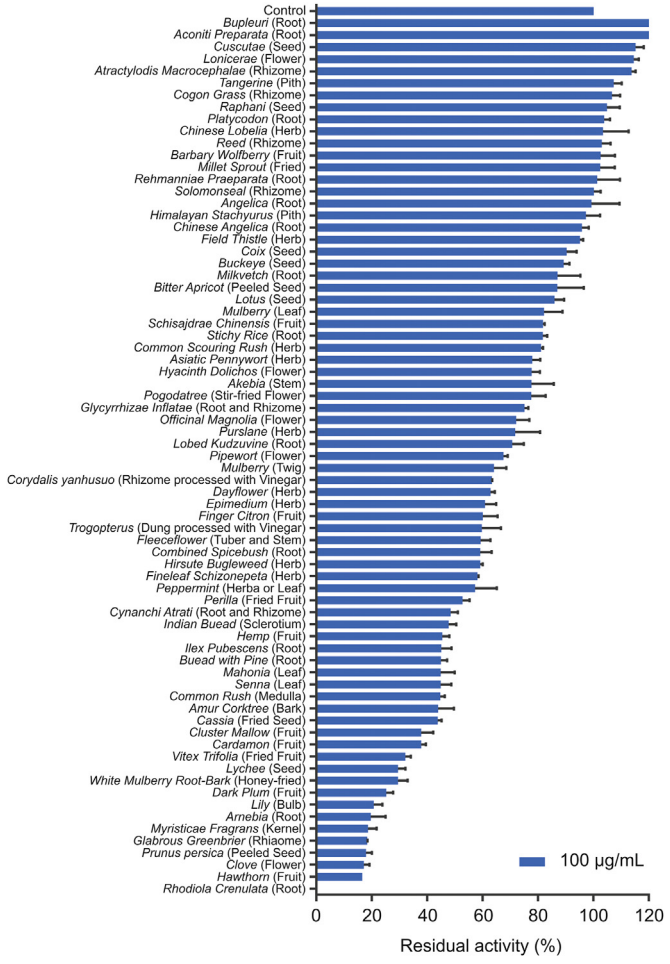

Fig. 1. The residual activities of all examined herbal medicines (100 μg/mL, final concentration) against human pancreatic lipase (hPL)-catalyzed 4-methylumbelliferyl oleate (4-MUO) hydrolysis. All data are shown as means ± SD (n = 3).

3.2. Identification of bioactive fractions of ERC with anti-hPL activity

Given that ERC contains numerous constituents, development of an efficient approach to identifying its constituents with anti-hPL activity is necessary. To this end, we adopted an integrated strategy, involving bioactivity assays and the LC-MS-guided fractionation method. Initially, an LC-Q-TOF-MS/MS-based chemical profiling assay was established for the separation and identification of the ERC constituents. Total ion chromatographs of ERC in both negative and positive ion modes are shown in Figs. S5 and S6, respectively. Reverse-phase LC fractions of ERC were collected at 2.5 min intervals (from 0 to 50 min), and the inhibitory effects of the eluents against hPL were analyzed. The results demonstrated that nine fractions (retention time (t_R) = 12.5–35 min) showed strong anti-hPL activity (Fig. 2), and all constituents of these nine fractions were identified by coupling LC with diode-array detection (LC-DAD) and LC-Q-TOF-MS/MS. Table S1 lists the bioactive

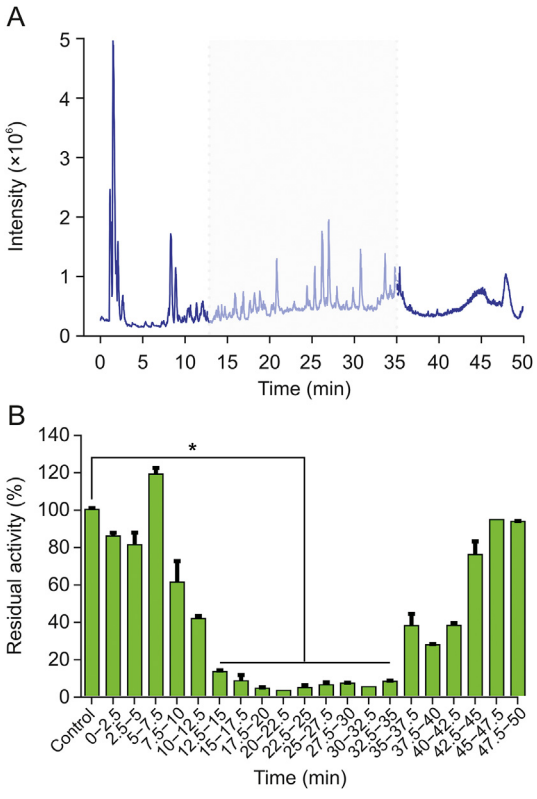

Fig. 2. (A) The total ion chromatogram (TIC) of the root extract of *Rhodiola crenulata* (ERC) obtained using LC-Q-TOF-MS/MS in negative ion mode. (B) The corresponding hPL residual activities of liquid chromatography fractions collected at 2.5 min intervals. *P < 0.0001 versus the control group.

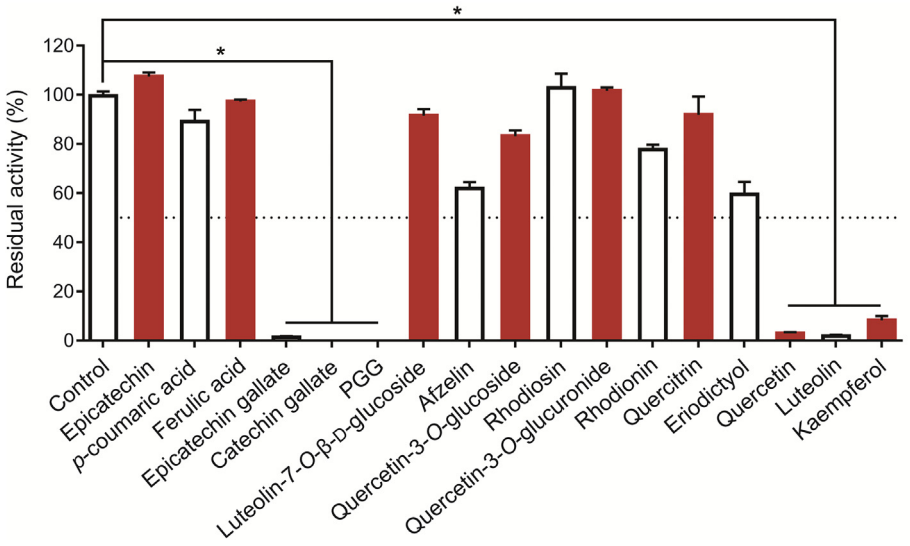

Fig. 3. The inhibitory effects of 17 constituents (100 μM, final concentration) in ERC against hPL. All data are shown as means ± SD ($n = 2$). *$P < 0.0001$ versus the control group. PGG: 1,2,3,4,6-penta-*O*-galloyl-β-D-glucopyranose.

fractions containing at least 35 compounds, which were initially characterized based on t_R and comparisons with the tandem mass spectrometry (MS/MS) spectra of selected standards, referenced from an in-house natural product MS/MS spectra database (Figs. S7–S76).

3.3. Anti-hPL activities of the selected ERC constituents

To further validate the bioactive constituents in ERC, seventeen commercially available constituents in the bioactive fractions of ERC are collected. And their inhibitory potentials against hPL-catalyzed 4-MUO hydrolysis were assayed at a final concentration of 100 μM. Among these constituents, six compounds showed strong anti-hPL activity, with residual activities of less than 50% (Fig. 3), for which the dose-dependent inhibition curves and pIC_{50} values were subsequently plotted and calculated, respectively (Fig. 4 and Table 1). The results clearly revealed that PGG and CG had the most potent anti-hPL activity ($pIC_{50}>7$), with pIC_{50} values of 7.59 ± 0.03 and 7.68 ± 0.23, respectively. Among the other constituents, ECG, quercetin, luteolin, and kaempferol showed strong to moderate hPL inhibition, with pIC_{50} values of 6.79 ± 0.02, 6.42 ± 0.13, 6.11 ± 0.06, and 4.56 ± 0.03, respectively. These findings demonstrated that ERC contains at least six naturally ocurring hPL inhibitors, among which PGG and CG are the most potent hPL inhibitors identified from ERC.

3.4. Inhibition kinetics of PGG and CG against hPL

To further elucidate the inhibitory mechanisms of the two newly identified naturally occurring hPL inhibitors (PGG and CG) against hPL, the inhibition kinetics and modes of PGG and CG against hPL were characterized by performing a series of inhibition kinetic assays. Inhibition kinetics plots, Lineweaver-Burk plots, and secondary plots of PGG and CG indicated that these two natural compounds potently inhibited hPL in non-competitive mode, with apparent inhibition constants (K_i) of 0.012 and 0.082 μM, respectively (Fig. 5 and Table S2). Interestingly, this putative inhibitory mechanisms (non-competitive) of PGG and CG against hPL differ from that of orlistat (Fig. S77), a marketed irreversible hPL inhibitor (Fig. 6).

3.5. Simulation of the docking between PGG/CG and hPL

In order to determine the binding modes and the molecular mechanisms of the two potent hPL inhibitors in ERC, docking simulations of PGG and CG into hPL were carried out. First, the ligand-binding cavities and the ligandability of each cavity in hPL (PDB ID: 1LPA) were predicted using CavityPlus (www.pkumdl.cn/cavityplus), an interactive server platform. As shown in Fig. S78, four potential ligand-binding cavities (cavities -1, -2, -3 and -4) with excellent ligandability (predicted average pKd>6.0) of hPL had been predicted by the CAVITY Module. Furthermore, the binding poses with the lowest binding energies were gained and the key interactions between the two newly identified ligands (PGG and CG) and hPL were carefully analyzed by whole-protein docking, while the affinity energies of PGG and CG on hPL were calculated as −9.4 and −9.0 kcal/mol, respectively. As depicted in Figs. 6 and S79, PGG was found to interact strongly with several amino acid residues in the A chain (Leu-41, Lys-42, Arg-44, and Arg-65) and B chain (Asp-331, Arg-337, Lys-367, and Glu-370) of hPL cavity-1 via hydrogen bond formation, and also interacted with Tyr-369 via π-π interactions. Similarly, CG formed hydrogen bonds with several key amino acid residues (Asn-212, Leu-213, Ile-241, Phe-258, and Ala-259) in cavity-4, and also interacted with Lys-238 (via alkyl interactions). These observations could partially explain the binding modes and sites of the interactions of PGG and CG with hPL.

4. Discussion

Herbal therapies are widely utilized for preventing and treating obesity and obesity-associated disorders in many countries, owing to their good safety profiles and evident lipid-lowering and weight-loss effects [37–41]. However, in most cases, the active constituents of HMs and their molecular mechanisms of action are rarely reported. Herbal preparations typically contain hundreds of natural constituents, thereby making it extremely difficult to identify the key active compounds in these complex mixtures. Accordingly, it is highly desirable to establish efficient approaches for the detection and characterization of these key components, either by using interdisciplinary strategies or state-of-the-art techniques. Given

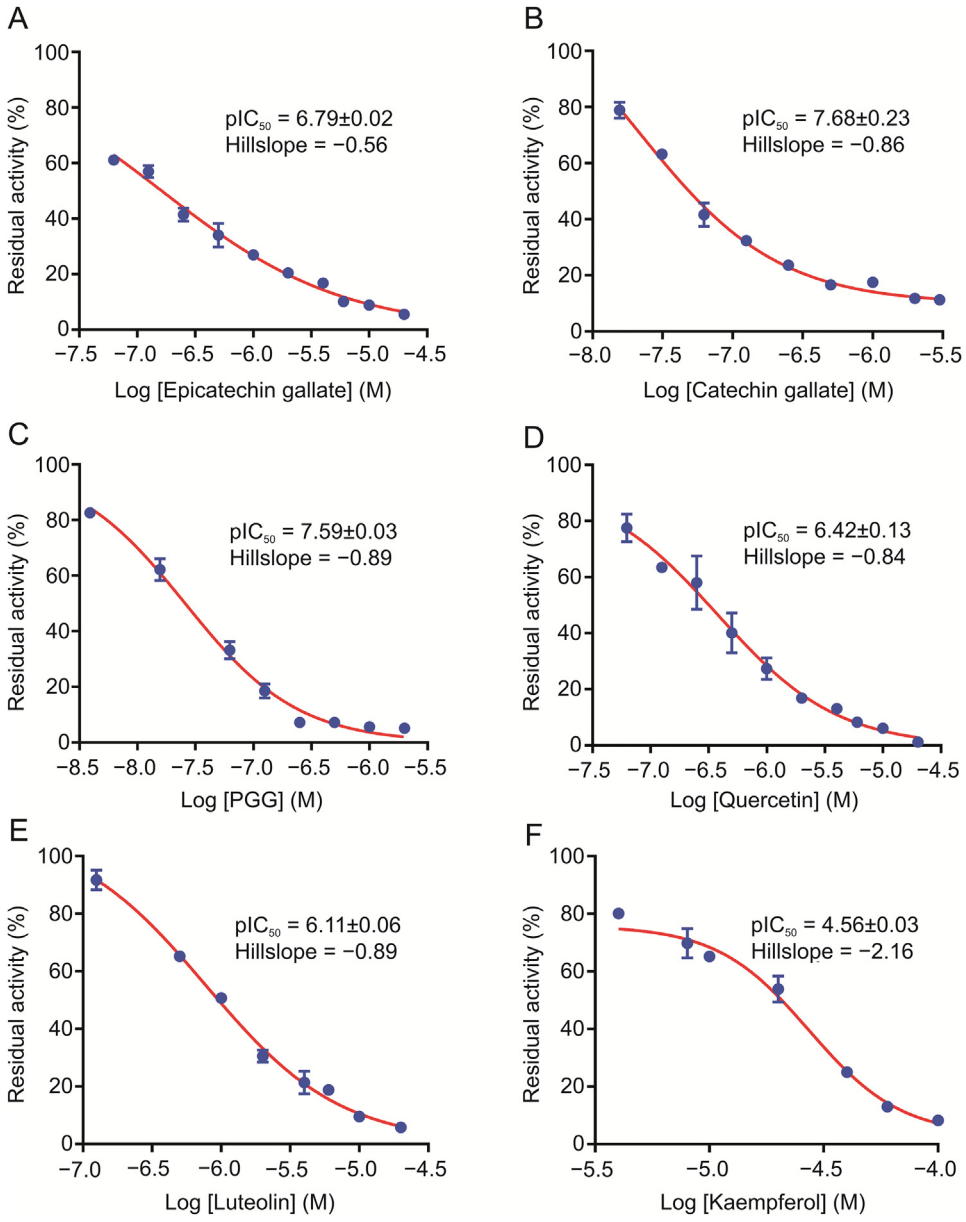

Fig. 4. Dose-inhibition curves of the activities of (A) epicatechin gallate (ECG), (B) catechin gallate (CG), (C) 1,2,3,4,6-penta-*O*-galloyl-β-D-glucopyranose (PGG), (D) quercetin, (E) luteolin, and (F) kaempferol against hPL. All data are shown as means ± SD ($n = 3$).

Table 1
The inhibitory effects of seventeen constituents in ERC against hPL-catalyzed 4-methylumbelliferyl oleate (4-MUO) hydrolysis.

No.	Compound	Molecular weight	pIC_{50}
1	Epicatechin	290.27	<4
2	*p*-coumaric acid	164.16	<4
3	Ferulic acid	194.18	<4
4	Epicatechin gallate	442.37	6.79 ± 0.02
5	Catechin gallate	442.37	7.68 ± 0.23
6	1,2,3,4,6-penta-*O*-galloyl-β-D-glucopyranose (PGG)	940.68	7.59 ± 0.03
7	Luteolin-7-*O*-β-D-glucoside	448.38	<4
8	Afzelin	432.38	<4
9	Quercetin-3-*O*-glucoside	464.38	<4
10	Rhodiosin	610.52	<4
11	Quercetin-3-*O*-glucuronide	478.36	<4
12	Rhodionin	448.38	<4
13	Quercitrin	448.38	<4
14	Eriodictyol	288.25	<4
15	Quercetin	302.24	6.42 ± 0.13
16	Luteolin	286.24	6.11 ± 0.06
17	Kaempferol	286.24	4.56 ± 0.03
Positive inhibitor	Orlistat [a]	495.74	7.98 ± 0.02

[a] Orlistat (a marketed hPL inhibitor) was used as the positive hPL inhibitor.

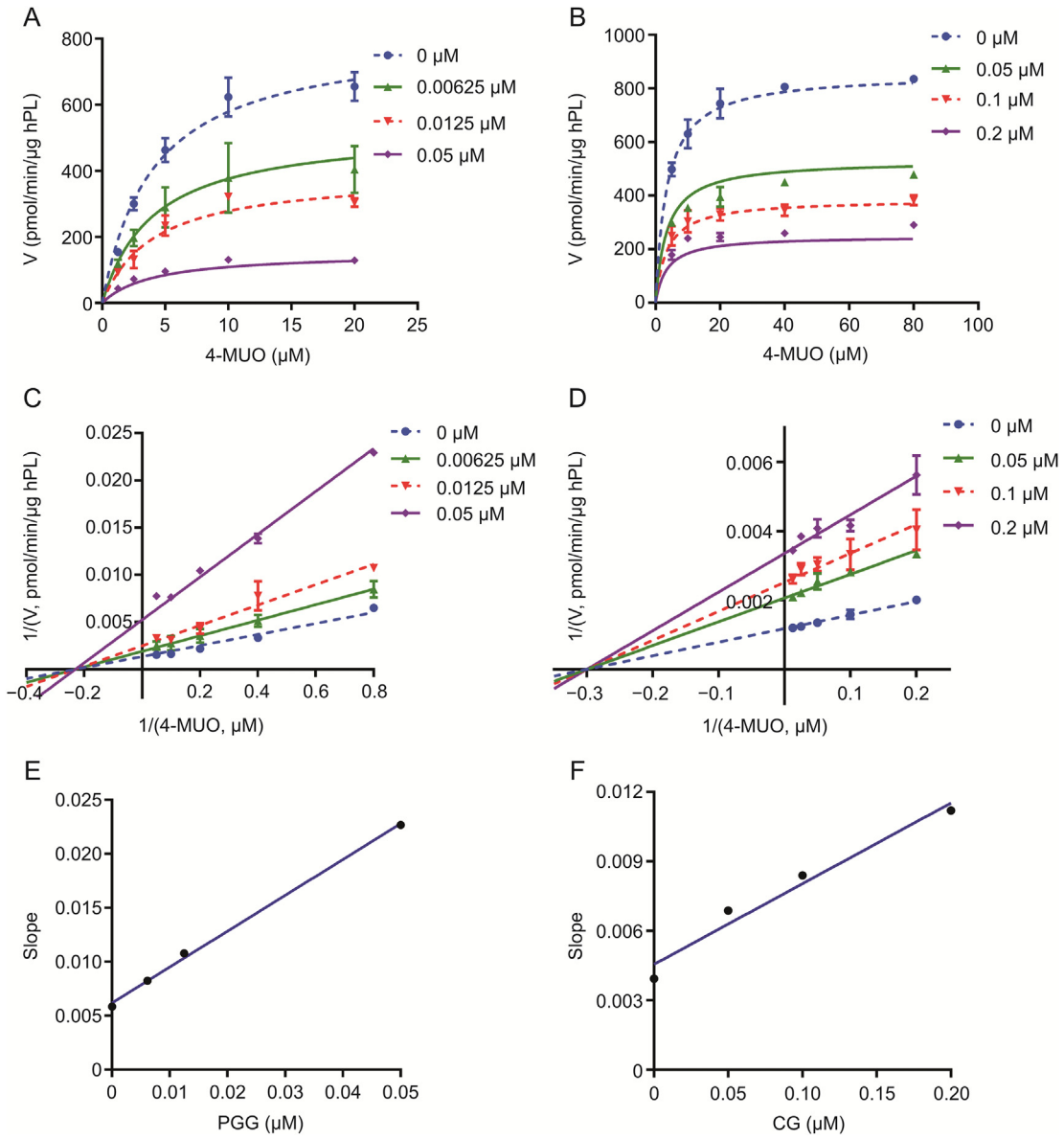

Fig. 5. Inhibition kinetics of 1,2,3,4,6-penta-*O*-galloyl-β-D-glucopyranose (PGG) and catechin gallate (CG) against hPL. Left: (A) The inhibition kinetic plots, (C) Lineweaver-Burk plots, and (E) the secondary plots of PGG against hPL-catalyzed 4-MUO hydrolysis. Right: (B) The inhibition kinetic plots, (D) Lineweaver-Burk plots, and (F) the secondary plots of CG against hPL-catalyzed 4-MUO hydrolysis. All data are shown as means ± SD ($n = 2$).

that most of the natural constituents found in HMs cannot be absorbed into the circulatory system and the majority of the absorbed natural ingredients can be readily metabolized by hepatic drug-metabolizing enzymes, it is assumed that these natural constituents are more likely to exert their lipid-lowering and weight-loss effects via targeting certain key therapeutic targets in the gastrointestinal tract [42,43]. In view of the fact that hPL is a validated therapeutic target for the regulation of lipid metabolism in the gastrointestinal tract, the discovery of potent anti-hPL constituents in HMs will predictably contribute to gaining a better understanding of the lipid-lowering or weight-loss effects of these compounds. To this end, we developed a practical and efficient research strategy, by integrating bioactivity-guided fractionation, chemical profiling, and biochemical assays, to characterize the key active constituents in HMs with strong anti-hPL activities.

In this study, following screening of the inhibition of 73 HMs against hPL, we found that ERC was the strongest hPL inhibitor, which contributed to further exploration of key active substances in this herbal medicine responsible for hPL inhibition. Chemical profiling revealed that ERC contains more than 50 natural constituents, while 35 constituents were identified from the bioactive LC fractions ($t_R = 12.5–35$ min) of this herbal extract. Inhibition assays and inhibition kinetic analyses clearly demonstrated that two newly identified natural constituents (PGG and CG) were potent non-competitive inhibitors of hPL ($K_i < 0.1$ μM). In addition to these two potent naturally occurring hPL inhibitors, other constituents in ERC including ECG, quercetin, luteolin, and kaempferol exhibited strong to moderate hPL inhibition activity. These findings offer convincing evidence to support the anti-obesity and the lipid-lowering activities of ERC. Interestingly, we also found that a pair of conformational isomers, namely, CG and ECG, had notably different anti-hPL potencies, with pIC_{50} values of 7.68 and 6.79, respectively. To establish the factors contributing to the differential inhibitory potency of these two isomers against hPL, the binding energies and the key interactions of CG and ECG

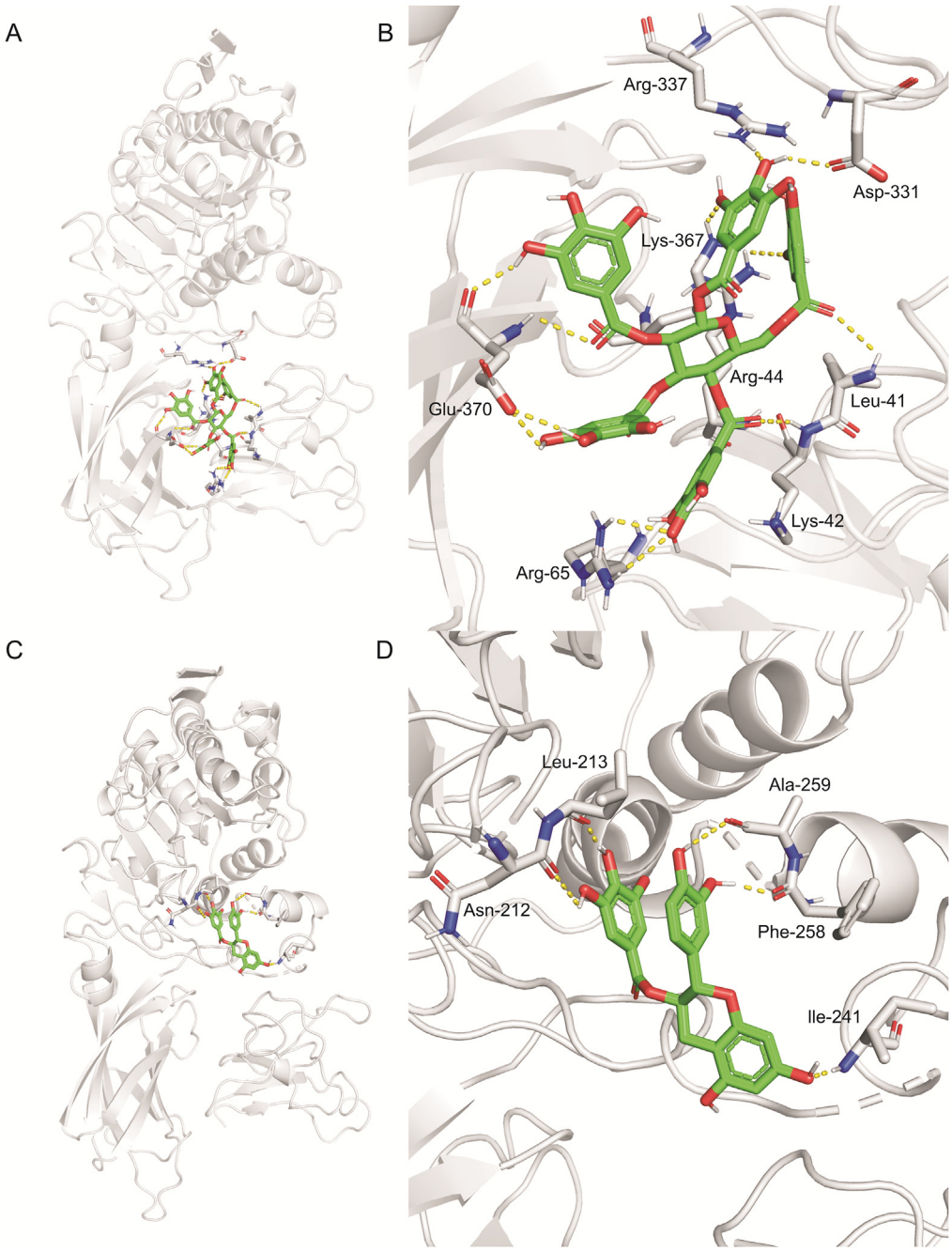

Fig. 6. An equilibrium (A and C) stereo overview and (B and D) detailed view of hPL docked with (A and B) PGG and (C and D) catechin gallate in protein binding cavities-1 and -4, respectively.

on hPL were carefully investigated based on docking simulations. The results clearly revealed that CG and ECG preferred to bind on hPL at cavity-4 via hydrogen bond interactions (Fig. S80), with corresponding high affinity energies of −9.0 and −8.0 kcal/mol, respectively, which indicates that CG can form a more stable conformation with hPL than ECG. Accordingly, this may provide at least a partial explanation for why CG displayed more potent hPL inhibitory activity in comparison with ECG. It is worth noting that CG and ECG are also major constituents of a variety of teas (such as green tea), which means that drinking tea is conducive to reducing lipid deposition in the human body.

As an edible herb and given its wide-ranging beneficial effects, including anti-oxidative, anti-inflammatory, and antibacterial activities and endocrine system regulatory function, *R. crenulata* has been used as a functional food in Asian countries [44,45]. In this regard, the findings of previous studies revealed that ERC and its constituents can regulate glycolipid metabolism by targeting a range of targets or pathways, but none of these studies were focused on the blocking of the activities of digestive enzymes (such as PL) in the gastrointestinal system [29,46–49]. Current research revealed that both ERC and its certain constituents display strong anti-hPL activity, suggesting hPL is a crucial target of ERC for preventing and treating obesity or obesity-related disorders. Following oral administration, ERC and its constituents can directly bind on hPL in the gastrointestinal system, which in turn, blocks lipid absorption. Notably, previous studies had reported that some

constituents in ERC (such as ECG, quercetin, and luteolin) display strong inhibitory effects against α-glucosidase [50–52], another key digestive enzyme in the gastrointestinal system associated with glucose absorption [53,54]. Consequently, it is conceivable that ERC or some constituents in ERC can be further developed as anti-obesity herbal medicines or agents via targeting multi-therapeutic target in the gastrointestinal system (at least hPL and α-glucosidase), which in turn, reduces both lipid and glucose absorption and improves insulin sensitivity.

5. Conclusion

In summary, this study reported a practical strategy for identifying and characterizing the key anti-obesity constituents of HMs, via integrating bioactivity-guided fractionation, LC-Q-TOF-MS/MS based chemical profiling, and hPL inhibition assays. Our findings clearly revealed that nine reverse-phase liquid chromatography fractions (t_R = 12.5–35 min) from ERC contained bioactive constituents with potent anti-hPL activities, which were subsequently identified and assessed using LC-Q-TOF-MS/MS analyses and hPL inhibition assays, respectively. Among all identified anti-hPL constituents, PGG and CG were identified as the two most potent hPL inhibitors, with pIC_{50} values of 7.59 ± 0.03 and 7.68 ± 0.23, respectively. Inhibition kinetics analyses demonstrated that PGG and CG potently inhibited hPL in a non-competitive manner, with K_i values of 0.012 and 0.082 μM, respectively. Subsequent docking simulation analyses indicated that PGG and CG can strongly interact with hPL via tight binding in two allosteric pockets (cavities 1 and 4), rather than the catalytic pocket of hPL. Collectively, our findings enabled us to identify the key anti-obesity constituents in ERC and to elucidate the inhibitory mechanisms of two potent hPL inhibitors in this herbal medicine, which provides convincing evidence in support of the anti-obesity and the lipid-lowering activities of ERC. In addition, the strategy adopted in this study could be applied to discover the bioactive constituents (especially for enzyme modulators) in other herbal medicines.

CRediT author statement

Li-Juan Ma: Data curation, Writing - Original draft preparation; **Xu-Dong Hou:** Investigation, Methodology, Validation, Data curation, Writing - Original draft preparation; **Xiao-Ya Qin:** Methodology, Data curation; **Rong-Jing He:** Methodology, Data curation; **Hao-Nan Yu:** Investigation; **Qing Hu:** Methodology; **Xiao-Qing Guan:** Formal analysis; **Shou-Ning Jia:** Resources, Funding acquisition; **Jie Hou:** Writing - Original draft preparation, Reviewing and Editing; **Tao Lei:** Funding acquisition; **Guang-Bo Ge:** Conceptualization, Supervision, Writing - Reviewing and Editing, Project administration.

Declaration of competing interest

The authors declare that there are no conflicts of interest.

Acknowledgments

This work was supported by the National Natural Science Foundation of China (Grant Nos.: 82160739, 81922070, 81973286, and 81973393), Sailing Special Project of Shanghai Rising-Star Program (Grant No.: 22YF1441500), Program for Innovative Leading Talents of Qinghai Province (2018 & 2019), Innovation Team and Talents Cultivation Program of National Administration of Traditional Chinese Medicine (Grant No.: ZYYCXTD-D-202004), Shanghai Science and Technology Innovation Action Plans (Grant Nos.: 20S21901500 and 20S21900900) supported by the Shanghai Science and Technology Committee, Project of the National Multidisciplinary Innovation Team of Traditional Chinese Medicine supported by the National Administration of Traditional Chinese Medicine, Key R&D and Transformation Science and Technology Cooperation Project of Qinghai Province (Grant No.: 2019-HZ-819), and Basic Public Welfare Research Program of Zhejiang Province (Grant No.: LGF22H280012). Furthermore, we are grateful to Zhou Yang (Shanghai Standard Technology Co., Ltd., Shanghai, China) for the contribution in the field of MS/MS analysis.

Appendix A. Supplementary data

Supplementary data to this article can be found online at https://doi.org/10.1016/j.jpha.2022.04.002.

References

[1] A. Afshin, M.H. Forouzanfar, M.B. Reitsma, et al., Health effects of overweight and obesity in 195 countries over 25 years, N. Engl. J. Med. 377 (2017) 13–27.
[2] G.M. Singh, G. Danaei, F. Farzadfar, et al., The age-specific quantitative effects of metabolic risk factors on cardiovascular diseases and diabetes: a pooled analysis, PLoS One 8 (2013), e65174.
[3] G. Seravalle, G. Grassi, Obesity and hypertension, Pharmacol. Res. 122 (2017) 1–7.
[4] B. Lauby-Secretan, C. Scoccianti, D. Loomis, et al., Body fatness and cancer–viewpoint of the IARC working group, N. Engl. J. Med. 375 (2016) 794–798.
[5] J.N. Keith, Pharmacotherapy in treatment of obesity, Gastroenterol. Clin. N. Am. 45 (2016) 663–672.
[6] P.J. Teixeira, M.M. Marques, Health behavior change for obesity management, Obes. Facts 10 (2017) 666–673.
[7] Y.-C. Chang, X. Liu, Q. Xu, et al., Current paradigm shifts in diet: a review of the Chinese traditional diet, Chin Med Cult 4 (2021) 99–106.
[8] V. Narayanaswami, L.P. Dwoskin, Obesity: current and potential pharmacotherapeutics and targets, Pharmacol. Ther. 170 (2017) 116–147.
[9] Y. Ding, Z. Gu, Y. Wang, et al., Clove extract functions as a natural fatty acid synthesis inhibitor and prevents obesity in a mouse model, Food Funct. 8 (2017) 2847–2856.
[10] Q.Y. Liu, Y.T. Wang, L.G. Lin, New insights into the anti-obesity activity of xanthones from *Garcinia mangostana*, Food Funct. 6 (2015) 383–393.
[11] H. Liu, M. Liu, Z. Jin, et al., Ginsenoside Rg2 inhibits adipogenesis in 3T3-L1 preadipocytes and suppresses obesity in high-fat-diet-induced obese mice through the AMPK pathway, Food Funct. 10 (2019) 3603–3614.
[12] Y. Rao, Q. Wen, R. Liu, et al., PL-S2, a homogeneous polysaccharide from *Radix Puerariae* lobatae, attenuates hyperlipidemia via farnesoid x receptor (FXR) pathway-modulated bile acid metabolism, Int. J. Biol. Macromol. 165 (2020) 1694–1705.
[13] C. Ren, Y. Zhang, W. Cui, et al., A polysaccharide extract of mulberry leaf ameliorates hepatic glucose metabolism and insulin signaling in rats with type 2 diabetes induced by high fat-diet and streptozotocin, Int. J. Biol. Macromol. 72 (2015) 951–959.
[14] Z. Zhang, M. Jiang, X. Wei, et al., Rapid discovery of chemical constituents and absorbed components in rat serum after oral administration of fuzi-lizhong pill based on high-throughput HPLC-Q-TOF/MS analysis, Chin. Med. 14 (2019), 6.
[15] L. Wang, X.Q. Guan, R.J. He, et al., Pentacyclic triterpenoid acids in *Styrax* as potent and highly specific inhibitors against human carboxylesterase 1A, Food Funct. 11 (2020) 8680–8693.
[16] Y.Q. Song, X.Q. Guan, Z.M. Weng, et al., Discovery of hCES2A inhibitors from glycyrrhiza inflata via combination of docking-based virtual screening and fluorescence-based inhibition assays, Food Funct. 12 (2021) 162–176.
[17] Y.Q. Wang, Z.M. Weng, T.Y. Dou, et al., Nevadensin is a naturally occurring selective inhibitor of human carboxylesterase 1, Int. J. Biol. Macromol. 120 (2018) 1944–1954.
[18] R.B. Birari, K.K. Bhutani, Pancreatic lipase inhibitors from natural sources: unexplored potential, Drug Discov, Today Off. 12 (2007) 879–889.
[19] L. Rajan, D. Palaniswamy, S.K. Mohankumar, Targeting obesity with plant-derived pancreatic lipase inhibitors: a comprehensive review, Pharmacol. Res. 155 (2020), 104681.
[20] Y.H. Jo, S.B. Kim, J.H. Ahn, et al., Xanthones from the stems of *Cudrania tricuspidata* and their inhibitory effects on pancreatic lipase and fat accumulation, Bioorg. Chem. 92 (2019), 103234.
[21] X.D. Hou, L.L. Song, Y.F. Cao, et al., Pancreatic lipase inhibitory constituents from Fructus psoraleae, chin, J. Nat. Med. 18 (2020) 369–378.
[22] X.D. Hou, X.Q. Guan, Y.F. Cao, et al., Inhibition of pancreatic lipase by the constituents in st. John's wort: in vitro and in silico investigations, Int. J. Biol. Macromol. 145 (2020) 620–633.
[23] X.D. Hou, G.B. Ge, Z.M. Weng, et al., Natural constituents from Cortex Mori Radicis as new pancreatic lipase inhibitors, Bioorg. Chem. 80 (2018) 577–584.
[24] P.K. Liu, Z.M. Weng, G.B. Ge, et al., Biflavones from *Ginkgo biloba* as novel pancreatic lipase inhibitors: inhibition potentials and mechanism, Int. J. Biol. Macromol. 118 (2018) 2216–2223.

[25] L. Zhang, J. Zheng, M. Ma, et al., Drug-guided screening for pancreatic lipase inhibitors in functional foods, Food Funct. 12 (2021) 4644–4653.
[26] G.Y. Xia, L.Y. Wang, J.F. Zhang, et al., Three new polyoxygenated bergamotanes from the endophytic fungus *Penicillium purpurogenum* IMM 003 and their inhibitory activity against pancreatic lipase, Chin. J. Nat. Med. 18 (2020) 75–80.
[27] V. Point, K.V. Pavan Kumar, S. Marc, et al., Analysis of the discriminative inhibition of mammalian digestive lipases by 3-phenyl substituted 1,3,4-oxadiazol-2(3H)-ones, Eur. J. Med. Chem. 58 (2012) 452–463.
[28] A. Abousalham, R. Verger, Egg yolk lipoproteins as substrates for lipases, Biochim. Biophys. Acta 1485 (2000) 56–62.
[29] J. Wang, X. Rong, W. Li, et al., *Rhodiola crenulata* root ameliorates derangements of glucose and lipid metabolism in a rat model of the metabolic syndrome and type 2 diabetes, J. Ethnopharmacol. 142 (2012) 782–788.
[30] Q. Hu, Z.-H. Tian, H.-N. Wang, et al., Rational design and development of a novel and highly specific near-infrared fluorogenic substrate for sensing and imaging of human pancreatic lipase in living systems, Sensor. Actuator. B Chem. 341 (2021), 130033.
[31] W. He, J.J. Wu, J. Ning, et al., Inhibition of human cytochrome P450 enzymes by licochalcone A, a naturally occurring constituent of licorice, Toxicol. Vitro 29 (2015) 1569–1576.
[32] W. Lei, D.D. Wang, T.Y. Dou, et al., Assessment of the inhibitory effects of pyrethroids against human carboxylesterases, Toxicol. Appl. Pharmacol. 321 (2017) 48–56.
[33] H. Xin, X.Y. Qi, J.J. Wu, et al., Assessment of the inhibition potential of licochalcone A against human UDP-glucuronosyltransferases, Food Chem. Toxicol. 90 (2016) 112–122.
[34] O. Trott, A.J. Olson, Autodock vina: improving the speed and accuracy of docking with a new scoring function, efficient optimization, and multithreading, J. Comput. Chem. 31 (2010) 455–461.
[35] J. Hermoso, D. Pignol, B. Kerfelec, et al., Lipase activation by nonionic detergents. the crystal structure of the porcine lipase-colipase-tetraethylene glycol monooctyl ether complex, J. Biol. Chem. 271 (1996) 18007–18016.
[36] Y. Xu, S. Wang, Q. Hu, et al., Cavityplus: a web server for protein cavity detection with pharmacophore modelling, allosteric site identification and covalent ligand binding ability prediction, Nucleic Acids Res. 46 (2018) W374–W379.
[37] J. Lan, Y. Zhao, F. Dong, et al., Meta-analysis of the effect and safety of berberine in the treatment of type 2 diabetes mellitus, hyperlipemia and hypertension, J. Ethnopharmacol. 161 (2015) 69–81.
[38] K. He, S. Kou, Z. Zou, et al., Hypolipidemic effects of alkaloids from *Rhizoma coptidis* in diet-induced hyperlipidemic hamsters, Planta Med. 82 (2016) 690–697.
[39] C.J. Zhou, S. Huang, J.Q. Liu, et al., Sweet tea leaves extract improves leptin resistance in diet-induced obese rats, J. Ethnopharmacol. 145 (2013) 386–392.
[40] M. Zhong, X. Song, X. Zhang, et al., Treatment of microcirculation dysfunction in type 2 diabetic mellitus with shenqi compound prescription: a protocol of systematic review and meta-analysis of randomized clinical trials, Medicine (Baltim.) 99 (2020), e22347.
[41] B. Tian, J. Zhao, X. Xie, et al., Anthocyanins from the fruits of *Lycium ruthenicum* Murray improve high-fat diet-induced insulin resistance by ameliorating inflammation and oxidative stress in mice, Food Funct. 12 (2021) 3855–3871.
[42] W. Zhou, L.Q. Di, J.J. Shan, et al., Intestinal absorption of forsythoside A in different compositions of Shuang-Huang-Lian, Fitoterapia 82 (2011) 375–382.
[43] Z.R. Dai, J. Ning, G.B. Sun, et al., Cytochrome P450 3A enzymes are key contributors for hepatic metabolism of bufotalin, a natural constitute in Chinese medicine Chansu, Front. Pharmacol. 10 (2019), 52.
[44] H. Tao, X. Wu, J. Cao, et al., *Rhodiola* species: a comprehensive review of traditional use, phytochemistry, pharmacology, toxicity, and clinical study, Med. Res. Rev. 39 (2019) 1779–1850.
[45] T. Zheng, F. Bian, L. Chen, et al., Beneficial effects of *Rhodiola* and salidroside in diabetes: potential role of AMP-activated protein kinase, Mol. Diagn. Ther. 23 (2019) 489–498.
[46] F. Li, H. Tang, F. Xiao, et al., Protective effect of salidroside from *Rhodiolae Radix* on diabetes-induced oxidative stress in mice, Molecules 16 (2011) 9912–9924.
[47] C. Yuan, Y. Jin, L. Yao, et al., *Rhodiola crenulata* root extract ameliorates fructose-induced hepatic steatosis in rats: association with activating autophagy, Biomed. Pharmacother. 125 (2020), 109836.
[48] W.J. Lee, H.H. Chung, Y.Z. Cheng, et al., *Rhodiola*-water extract induces beta-endorphin secretion to lower blood pressure in spontaneously hypertensive rats, Phytother Res. 27 (2013) 1543–1547.
[49] T. Zheng, X. Yang, W. Li, et al., Salidroside attenuates high-fat diet-induced nonalcoholic fatty liver disease via ampk-dependent TXNIP/NLRP3 pathway, Oxid. Med. Cell. Longev. (2018), 8597897.
[50] B.W. Zhang, X. Li, W.L. Sun, et al., Dietary flavonoids and acarbose synergistically inhibit alpha-glucosidase and lower postprandial blood glucose, J. Agric. Food Chem. 65 (2017) 8319–8330.
[51] Z. Wang, S. Peng, M. Peng, et al., Adsorption and desorption characteristics of polyphenols from eucommia ulmoides Oliv. Leaves with macroporous resin and its inhibitory effect on alpha-amylase and alpha-glucosidase, Ann. Transl. Med. 8 (2020), 1004.
[52] M. Yilmazer-Musa, A.M. Griffith, A.J. Michels, et al., Grape seed and tea extracts and catechin 3-gallates are potent inhibitors of alpha-amylase and alpha-glucosidase activity, J. Agric. Food Chem. 60 (2012) 8924–8929.
[53] S.D. Kim, Alpha-glucosidase inhibitor from *Buthus martensi* karsch, Food Chem. 136 (2013) 297–300.
[54] N. Pantidos, A. Boath, V. Lund, et al., Phenolic-rich extracts from the edible seaweed, ascophyllum nodosum, inhibit α-amylase and α-glucosidase: potential anti-hyperglycemic effects, J. Funct.Foods 10 (2014) 201–209.